Thin liquid films on rough or heterogeneous solids

Mark O. Robbins
Department of Physics and Astronomy, Johns Hopkins University, Baltimore, Maryland 21218 and Institute for Theoretical Physics, University of California, Santa Barbara, California 93106

David Andelman
School of Physics and Astronomy, Raymond and Beverly Sackler Faculty of Exact Sciences, Tel Aviv University, Ramat Aviv 69978, Tel Aviv, Israel and Institute for Theoretical Physics, University of California, Santa Barbara, California 93106

Jean-François Joanny
Institut Charles Sadron, 6 rue Boussingault, 67083 Strasbourg CEDEX, France
(Received 1 October 1990)

We study the conformation of thin liquid films on rough or heterogeneous solid substrates. The liquid-substrate interaction dominates for sufficiently thin films, and heterogeneity roughens the liquid interface. As the film thickens, surface tension becomes increasingly important, and the liquid interface flattens. A general equation for the equilibrium interface shape is derived. Analytic results are obtained in the limit of weak disorder for rough or self-affine surfaces as well as chemically heterogeneous solids. The effect of disorder depends strongly on the wave vector. Fluctuations at scales smaller than the film thickness or a "healing length" ξ produce little roughness. At larger wavelengths, the film conforms to the local fluctuations. Exact numerical solutions of the general equation are presented for surfaces with square grooves. These confirm the qualitative predictions of the analytic theory, and are in quantitative agreement when the depth of the grooves is small. The variation of roughness with film thickness, as well as the calculated adsorption isotherms, are compared to recent experimental results. We show that previously measured isotherms can be reproduced by corrugated surfaces with a single characteristic length scale, and do not necessarily imply that the surfaces studied were self-similar.

I. INTRODUCTION

Studies of interfacial phenomena generally focus on ideal flat and homogeneous surfaces.[1–4] However, most surfaces of experimental or technological interest are both rough and chemically heterogeneous. This disorder can have dramatic effects on various physical processes.

For a liquid partially wetting a solid surface, i.e., showing a finite contact-angle between the solid surface and the liquid-vapor interface, heterogeneity is known to produce contact-angle hysteresis.[5,6] Namely, the measured contact angle depends on the history of the liquid interface. The surface heterogeneity is analogous to a random field[7] that pins the solid-liquid-vapor triple line, causing it to have many metastable states.[8–10]

In this paper we discuss the other limit of *complete* wetting where the liquid spreads on the solid surface and forms a thin *but continuous* film with an average thickness in the mesoscopic range (a few angstroms to a micrometer). At these scales the long-range component of molecular interactions must be included explicitly. Heterogeneity and roughness of the solid surface induce fluctuations in the liquid interface above it. We present general equations describing these fluctuations, and analytic and numerical solutions for specific cases.[11,12]

Three examples of experimentally realizable wetting films are illustrated in Fig. 1: (i) a thin liquid film in equilibrium with its undersaturated vapor [Fig. 1(a)]; (ii) a liquid film on a horizontal plate located at height h above a liquid reservoir [Fig. 1(b)]; (iii) a nonvolatile liquid whose total volume is conserved [Fig. 1(c)]. In the

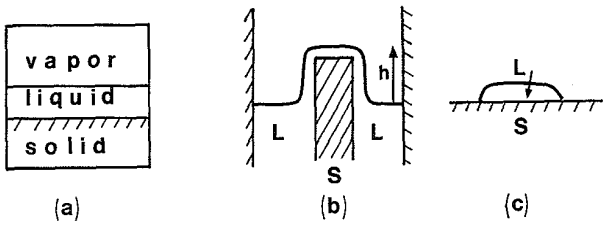

FIG. 1. (a) A liquid film on a horizontal plate in equilibrium with its undersaturated vapor. (b) A liquid film at a height h above a reservoir. (c) A nonvolatile liquid drop of constant volume spreading on a solid.

last two cases the vapor phase could instead be another immiscible liquid. Other wetting situations to which our study can apply are precursor films formed ahead of advancing liquid fronts, or even liquid films ascending on a vertical plate (Rollin films).[4]

Several recent experiments have measured the effects of roughness and heterogeneity on thin liquid films.[13–17] In one experiment by Garoff *et al.*,[13] x-ray reflection from a synchrotron source was used to analyze thin wetting films on glass surfaces which were neither ideally flat nor chemically pure. The measured rms roughness of the glass substrate was 7.2 Å. The roughness of the water-air interface decreased from 5.2 Å in 14-Å-thick films to about 3.6–4.2 Å in 70–100-Å films. In contrast, the thermal roughness of a bulk water surface[18] is only 3.2 Å and decreases with film thickness.[13] Studies of the diffuse scattering showed conclusively that the additional roughness of the water-air film was correlated with the roughness of the underlying substrate.[13]

In another experiment, Beaglehole[15] has studied the wetting of polydimethylsiloxane (PDMS) drops on etched glass, fused silica, and mica surfaces by the ellipsometry technique.[16] With a special technique of microscopic imaging ellipsometry, the average thickness and local fluctuations in the liquid thickness were measured in the precursor film close to the edge of the advancing PDMS drop. Furthermore, it was reported[15] that these thickness fluctuations were roughly inversely proportional to the local film thickness.

Finally, information about the structure of nonideal solid surfaces can also be obtained from adsorption experiments.[19] Recently deviations from adsorption isotherms on flat surfaces were used to infer that flash-deposited Ag films have fractal surface structure.[17]

The layout of our paper is as follows. In Sec. II we develop the theoretical formalism needed for the calculation of the equilibrium film profile. In Sec. III we discuss wetting of rough solid surfaces within a linear response theory and a local Deryagin approximation. Then, in Sec. IV, we present numerical results for periodically corrugated solid surfaces which confirm our analytical findings. Surfaces which are rough on all length scales—self-affine or self-similar surfaces—are discussed in Sec. V. The use of adsorption isotherms to identify such surfaces is critically reviewed. Finally, we discuss wetting of heterogeneous solids in Sec. VI. Two types of heterogeneity are considered in detail: layered and columnar materials. Conclusions and connections with experiments are presented in Sec. VII.

II. EQUILIBRIUM INTERFACE SHAPE

We derive the equations for a liquid-vapor interface (called the liquid surface below) and then discuss how they are modified for a liquid-liquid interface. As shown in Fig. 2, the coordinate system is oriented with the z axis perpendicular to the undeformable solid surface. We consider rough or self-affine surfaces without overhangs.[20] Hence the solid and liquid surfaces can be represented by single-valued functions $\zeta_S(\mathbf{x})$ and $\zeta_L(\mathbf{x})$ of the position $\mathbf{x}$ in the x-y plane. The origin in the z direction is chosen so that $\langle\zeta_S\rangle = \int d^2x\,\zeta_S(\mathbf{x}) = 0$.

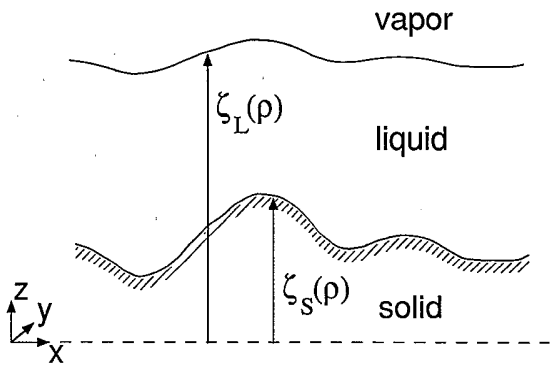

FIG. 2. A continuous liquid film covering a rough solid surface. The liquid and solid surfaces are at height $\zeta_L(\rho)$ and $\zeta_S(\rho)$, respectively, above the $z = 0$ reference plane.

The wetting film can coexist with undersaturated vapor because the extra attractive potential from the solid lowers the chemical potential of the liquid near the solid. This attraction is frequently expressed as a positive disjoining pressure Π_d on the liquid interface.[1–4] Following such treatments we express Π_d in terms of two-body interactions $u_{IJ}(\mathbf{r},\mathbf{r}')$ which equal the interaction energy between unit volumes at $\mathbf{r}$ and $\mathbf{r}'$ of phases I and J. Here $I = S$, L, and V denote solid, liquid, and vapor phases, respectively. If the phases are homogeneous (Secs. III–V), $u_{IJ}(\mathbf{r},\mathbf{r}')$ only depends on $|\mathbf{r}-\mathbf{r}'|$. In Sec. VI we consider the case of heterogeneous solids where u_{SJ} depends on both coordinates.

If the vapor is much less dense than the liquid, its interactions with the other phases can be neglected. The solid-liquid interaction lowers the liquid chemical potential per unit volume at a point $\mathbf{r} = (\mathbf{x}, \zeta_L(\mathbf{x}))$ on the liquid interface by

$$\Pi_d(\mathbf{x},\zeta_L(\mathbf{x})) = \int_{\text{solid}} d\mathbf{r}'\, w(\mathbf{r},\mathbf{r}')\,, \tag{1}$$

where $w(\mathbf{r},\mathbf{r}') \equiv u_{LL}(\mathbf{r},\mathbf{r}') - u_{LS}(\mathbf{r},\mathbf{r}')$ and the integral is over the entire solid region. On a flat, homogeneous solid, Π_d is independent of $\mathbf{x}$ and the constant equilibrium value of ζ_L is determined by equating Π_d to the chemical potential difference $\Delta\mu$ between unit volumes of liquid and vapor phases. One can interpret Π_d as the pressure confining the liquid. The larger the chemical potential difference, the larger Π_d is, and the thinner the film.

The surface of constant disjoining pressure above a disordered solid will be curved to reflect the variations in attraction from regions of different height or chemical composition. The liquid surface does not follow this curved surface exactly because of the surface tension γ. There is an extra Laplace pressure drop across a curved interface, $\gamma(\kappa_1+\kappa_2)$, where κ_1 and κ_2 are the principal

curvatures. In the context of liquid-vapor coexistence, the Laplace pressure reflects the fact that liquid condenses more readily in concave regions of the interface ($\kappa < 0$) than at convex regions because concave regions are surrounded by more liquid. Combining the Laplace pressure with the disjoining pressure, we find the general equation for the equilibrium interface profile:

$$\gamma \frac{\nabla^2 \zeta_L(\mathbf{x})}{[1+|\nabla \zeta_L(\mathbf{x})|^2]^{3/2}} + \Pi_d(\mathbf{x}, \zeta_L(\mathbf{x})) = \Delta\mu \,, \qquad (2)$$

where we have written the curvature explicitly in terms of gradients of ζ_L.

The form of the chemical potential difference $\Delta\mu$ in Eq. (2) is different for cases (i) – (iii) illustrated in Fig. 1. For case (i), $\Delta\mu = -\rho k_B T \ln(p/p_{\rm sat})$, where ρ is the density of the liquid phase, p is the vapor pressure, and $p_{\rm sat}$ is the saturated pressure. For case (ii), $\Delta\mu = \rho g h$ reflects the hydrostatic pressure where g is the gravitational acceleration. Finally, for case (iii), $\Delta\mu$ is a Lagrange multiplier associated with conservation of the total liquid volume.

Consider now the more general case where a second liquid L' replaces the vapor phase. The main difference is that above we have ignored the shift in the chemical potential per unit volume of the vapor phase because its density is generally negligible compared to that of the liquid. This is not possible if the phase is a second liquid. Subtracting the shift in the chemical potential of this liquid we get the same expression for Π_d, but with

$$w(\mathbf{r},\mathbf{r}') = u_{LL}(\mathbf{r},\mathbf{r}') + u_{SL'}(\mathbf{r},\mathbf{r}') - u_{LL'}(\mathbf{r},\mathbf{r}') - u_{SL}(\mathbf{r},\mathbf{r}'). \qquad (3)$$

For two-liquid systems the chemical potential difference may correspond to a Lagrange multiplier maintaining constant liquid volume, or to the chemical potential difference of a phase segregating out of a binary mixture.

We now specialize this result to several interesting cases. In Secs. III – V we consider rough surfaces where the only disorder is in ζ_S. In this case the solid is homogeneous and $w(\mathbf{r},\mathbf{r}') = w(|\mathbf{r}-\mathbf{r}'|)$. Then, in Sec. VI we consider heterogeneous solids with flat surfaces: $\zeta_S = 0$. Here the disorder is in w.

III. WETTING OF ROUGH SOLIDS

A. Linear approximation

As noted above, w only depends on the relative distance between two points. We change to cylindrical coordinates writing $\mathbf{r}' - \mathbf{r}$ as $(\boldsymbol{\rho}, z)$. Then the integral over $\mathbf{r}'$ in Eq. (1) is an integral over all $\boldsymbol{\rho}$ and over z between $-\infty$ and $\zeta_S(\mathbf{x}+\boldsymbol{\rho}) - \zeta_L(\mathbf{x})$. Using the spherical symmetry of w we can write

$$\Pi_d(\mathbf{x}, \zeta_L(\mathbf{x})) = \int d^2\rho \int_{\zeta_L(\mathbf{x})-\zeta_S(\mathbf{x}+\boldsymbol{\rho})}^{+\infty} dz\, w(\rho, z). \qquad (4)$$

In this section we simplify the expression for Π_d by expanding about a flat interface. The mean thickness of the film $\ell \equiv \langle \zeta_L - \zeta_S \rangle = \langle \zeta_L \rangle$, since the coordinates were chosen so $\langle \zeta_S \rangle = 0$. We expand Eqs. (2) and (4) assuming $|\zeta_L(\mathbf{x}) - \zeta_S(\mathbf{x}+\boldsymbol{\rho}) - \ell|/\ell$ and $|\nabla \zeta_L(\mathbf{x})|$ are small. The zeroth-order term gives a relation between the mean thickness and the chemical potential difference:

$$\Pi_d^0(\ell) = \Delta\mu, \qquad (5)$$

where Π_d^0 is the disjoining pressure for a flat substrate. The linear term gives

$$\xi^2 \nabla^2 \zeta_L(\mathbf{x}) = \zeta_L(\mathbf{x}) - \ell - \int d^2\rho\, K(\mathbf{x}-\boldsymbol{\rho})\, \zeta_S(\boldsymbol{\rho}), \qquad (6)$$

where $\xi(\ell)$ is a surface-tension- and thickness-dependent *healing length*,

$$\xi(\ell)^2 = \frac{\gamma}{\int d^2\rho\, w(\rho, \ell)}, \qquad (7)$$

and the kernel $K(\mathbf{x}, \ell)$ is

$$K(\mathbf{x}, \ell) = \frac{w(\mathbf{x}, \ell)}{\int d^2\rho\, w(\rho, \ell)}. \qquad (8)$$

Equation (6) is readily solved by Fourier transforming to $\tilde{f}(\mathbf{q}) = \int d^2x\, f(\mathbf{x}) e^{-i\mathbf{q}\cdot\mathbf{x}}$. One finds[21]

$$\tilde{\zeta}_L(\mathbf{q}) = \frac{\tilde{\zeta}_S(\mathbf{q})\, \tilde{K}(\mathbf{q})}{1 + q^2\xi^2}. \qquad (9)$$

Several general conclusions can be drawn from these equations. From Eq. (8) it is apparent that $\tilde{K}(0) = 1$. Also, since w is a decreasing function of $\boldsymbol{\rho}$, $\tilde{K}$ will decrease with increasing $\mathbf{q}$. Thus for sufficiently small $\mathbf{q}$ the liquid surface will follow the rough solid surface because the Lorentzian fall off is negligible and $\tilde{K}(q) \approx 1$ [Eq. (9)]. For larger $\mathbf{q}$, the response of the liquid surface is attenuated. The attenuation in Eq. (9) comes from two sources. The Lorentzian fall off with characteristic length ξ comes from the smoothing influence of surface tension. The decrease in $\tilde{K}$ for large $\mathbf{q}$ reflects the nonlocal nature of the interaction. A point on the liquid surface is nearly equidistant from the crests and troughs of deformations ζ_S with wavelength much smaller than ℓ. There is little energy to be gained by following such fluctuations.

As a specific example we consider the case of van der Waals interactions. van der Waals interactions are of fundamental importance in wetting phenomena because they occur universally and fall off more slowly at large distances than other interactions. For simple surfaces, the full Lifshitz theory of van der Waals interactions is well approximated by an inverse power-law pair potential.[1,22] Thus, throughout the paper we will focus on inverse power-law interactions,

$$w(r) = \frac{A}{\pi^2} \left(\frac{1}{r}\right)^{2m+2}, \qquad (10)$$

and in particular on nonretarded van der Waals interactions which correspond to $m = 2$. The factors of π in Eq. (10) are chosen so that A is the conventional Hamaker

constant.[1] In this case the integral over z in Eq. (4) can be calculated analytically:[11]

$$\Pi_d(\zeta_L) = \frac{3A}{8\pi^2}\int \frac{d^2\rho}{\rho^5}\left(\tan^{-1}\frac{\rho}{\eta} - \frac{5\eta\rho^3 + 3\eta^3\rho}{3(\rho^2+\eta^2)^2}\right), \tag{11}$$

where $\rho = |\boldsymbol{\rho}|$ and $\eta(\mathbf{x},\boldsymbol{\rho}) = \zeta_L(\mathbf{x}) - \zeta_S(\mathbf{x}+\boldsymbol{\rho})$ is introduced for convenience. As a check, it is easy to verify that when both interfaces are planar and parallel, Eq. (11) reduces to the usual result

$$\Pi_d^0 = \frac{A}{6\pi\ell^3}. \tag{12}$$

Making the linear approximation for inverse power potentials we find

$$\tilde{K}(q) = \frac{2}{\Gamma(m)}\left(\frac{q\ell}{2}\right)^m K_m(q\ell)\ , \quad \xi = \left(\frac{m\pi\gamma}{A}\right)^{1/2}\ell^m\ , \tag{13}$$

where K_m is the modified Bessel function of the second kind of order m and Γ is the Euler Γ function. For van der Waals interactions, we insert $m = 2$ in Eq. (13) and obtain

$$\xi = \frac{\ell^2}{a} \quad , \quad a = \left(\frac{A}{2\pi\gamma}\right)^{1/2} \quad . \tag{14}$$

Here a is a microscopic length determined by the relative strength of the surface tension and the interaction potential. Typical liquid-vapor surface tensions are $\gamma \sim 20$–70 dyn/cm and Hamaker constants for insulator-liquid-vapor systems are of order k_BT, giving $a \sim 1$ Å at room temperature.[1,2] For liquid-liquid interfaces both A and γ are smaller, but a is of the same order. For metal substrates, the Hamaker constant may be more than an order of magnitude larger.[23] Taking numbers for the experimentally studied[17] nitrogen on silver system we find $a = 12$ Å at $T = 77$ K.

At large $q\ell$, the modified Bessel function K_m in Eq. (13) decays as $K_m(q\ell) \sim (q\ell)^{-1/2}\exp(-q\ell)$. Thus, roughness at wavelengths less than ℓ is cut off exponentially,

$$\tilde{\zeta}_L(\mathbf{q})/\tilde{\zeta}_S(\mathbf{q}) \sim q^{-1/2}\ell^{-5/2}\exp(-q\ell). \tag{15}$$

The relative size of ξ and ℓ determines whether surface tension or film thickness acts first in cutting off long-wavelength surface fluctuations. From Eq. (14) we see that $\xi/\ell = \ell/a$ for $m = 2$. Thus for molecularly thin films, $\ell < a$, ξ is less than ℓ and the exponential dominates the damping of solid roughness. However, many of the approximations made in Sec. II break down in this limit.[24] For thicker films, $\ell > a$, ξ is greater than ℓ. The roughness is then damped by the Lorentzian for $q\xi > 1$ and the exponential factor only becomes important for larger q when $q\ell \gg 1$.

The power-law potential just discussed has no intrinsic length scale. Thus ℓ is the only length which can appear in $\tilde{K}$. Two examples of potentials with intrinsic scales, exponential and Gaussian interactions, are treated in the Appendix. The same qualitative behavior is observed. The only difference is that the length scale of the potential enters in the expressions for ξ and $\tilde{K}$.

B. Deryagin approximation

A number of recent papers[11,25–27] have calculated the interface configuration in the Deryagin approximation,[3,28,29] where the disjoining pressure at each point $\mathbf{x}$ is assumed to equal Π_d^0 for a smooth substrate with film thickness $\zeta_L(\mathbf{x})-\zeta_S(\mathbf{x})$. We now consider when such an approximation is valid, by comparing with the results obtained from the linear approximation.

Making the Deryagin approximation in Eq. (2) does not change the zeroth-order term in the roughness, Eq. (5). However, the linear term simplifies:

$$\xi^2\nabla^2\zeta_L(\mathbf{x}) = \zeta_L(\mathbf{x}) - \ell - \zeta_S(\mathbf{x}). \tag{16}$$

Thus, at this order, the Deryagin approximation is equivalent to setting K equal to a Dirac δ function.[11,30] This in turn implies that $\tilde{K} = 1$ for all q in Eq. (9), so that the film thickness determines the smoothing only through the dependence of the healing length on the thickness, $\xi \propto \ell^2$.

Comparing to our results for power-law and exponential potentials, we see that the Deryagin approximation is not accurate for $q\ell \gg 1$ where the nonlocal expressions produce exponentially decaying $\tilde{K}(q)$. This failure may not be crucial if $\xi > \ell$ (the usual case), and if $\tilde{\zeta}_S(q)$ is relatively large at $q\ell < 1$. In this case, the Lorentzian damping in Eq. (9) substantially eliminates the small-wavelength fluctuations and the liquid roughness will be dominated by the fluctuations at $q\xi < 1$. However, if the dominant undulations of the solid are at $q\ell \geq 1$, the Deryagin approximation is never accurate as shown in the following section.

Before turning to our numerical results we consider the effect of higher-order terms in the weak roughness expansion within the Deryagin approximation. The second-order term is just the second derivative of Π_d^0 times half the squared fluctuation in thickness. The mean of this term changes the relation between thickness and chemical potential. Eq. (5) becomes

$$\Pi_d^0(\ell)\left(1 + \langle(\zeta_L - \ell - \zeta_S)^2\rangle\frac{1}{2\Pi_d^0(\ell)}\frac{d^2\Pi_d^0(\ell)}{d\ell^2}\right) = \Delta\mu, \tag{17}$$

where $\langle(\zeta_L - \ell - \zeta_S)^2\rangle$ can be evaluated approximately using the linear approximation [Eq. (9)].

In the case of wetting films, the disjoining pressure is positive. Its magnitude decreases more slowly as ℓ increases, so the second derivative is positive definite. Then from Eq. (17) any roughness of the solid substrate acts to decrease the value of $\Pi_d^0(\ell)$ at fixed chemical potential and thus increases the average film thickness. This result is easy to understand. Because of the sharp falloff in Π_d^0, the extra attraction from "higher" pieces of the surface is

larger than the decrease in attraction from "lower" pieces of the surface.

IV. NUMERICAL SOLUTIONS FOR PERIODICALLY CORRUGATED SURFACES

The approximations described above break down as the solid roughness increases. We have solved Eq. (2) numerically to determine when errors become significant, and whether the qualitative predictions of the linear approximation are generally valid. To simplify the calculation we specialize to one-dimensional corrugations of the solid surface. If the x axis is chosen so that $\zeta_S = \zeta_S(x)$, the integrals over y and z can be evaluated analytically for power-law potentials.[31] We only quote the result for van der Waals interactions ($m = 2$):

$$\Pi_d(x,\zeta_L(x)) = \frac{A}{8\pi}\int \frac{dx'}{x'^4}\left(2 - \frac{\eta(3x'^2+2\eta^2)}{(x'^2+\eta^2)^{3/2}}\right), \qquad (18)$$

where $\eta = \zeta_L(x) - \zeta_S(x+x')$. The final integral over x' can be done analytically for some model surfaces, including the case where ζ_S is piecewise quadratic.

As a model surface, we consider a periodic square wave corrugation with period D and peak to peak amplitude H (Fig. 3). For power-law potentials, the solution for the interface only depends on the dimensionless parameters D/a, H/a, and ℓ/a. Figure 3(a) shows numerical solutions of Eqs. (2) and (18) for $D/a = 100$, $H/a = 5$, and Fig. 3(b) for $D/a = 10$, $H/a = 5$. As expected from the linear approximation, the liquid interface gets smoother as D decreases (q increases). In both cases the roughness of the interface only becomes comparable to that of the solid when $\xi = \ell^2/a \ll D/2$. For deep narrow grooves, Fig. 3(b), the film remains quite flat, $\zeta_L \approx \ell$, until the film thickness on the crests of the square wave reaches a well-defined value. Then there is a rapid change of shape. This occurs when the disjoining pressure on the crests is of order $2\gamma/D$, the capillary pressure required to penetrate the troughs.

One easily accessible experimental quantity is the coverage.[19] This is measured by weighing the film, and dividing by the projected surface area times the density. Since we consider surfaces without overhangs, the coverage is proportional to the mean film thickness ℓ. In experiments, the coverage is controlled by adjusting the pressure of an undersaturated vapor phase. The coverage exponent ϕ is defined by[32]

$$\Delta\mu \sim \ell^{-\phi}. \qquad (19)$$

For a flat surface $\Delta\mu = \Pi_d^0 = A/(6\pi\ell^3)$ [Eq. (5)], hence $\phi = 3$.

The variation of $\Delta\mu$ with ℓ for several geometries is shown in Fig. 4. As expected, the rough surface result approaches the flat surface one for films much thicker than the roughness. To estimate the leading correction to $\Delta\mu$ from Eq. (17) we note that for large ℓ, $\zeta_L \approx \ell$ and $\langle(\zeta_L - \zeta_S - \ell)^2\rangle \approx \langle\zeta_S^2\rangle = H^2/4$. For van der Waals interactions, $\Delta\mu \approx \Pi_d^0(\ell)(1 + 3H^2/2\ell^2)$. As shown in Fig. 4 (dashed line), this approximation works well at large ℓ. For thin films, $\xi < D/2$, the film follows the substrate and $\langle(\zeta_L - \zeta_S - \ell)^2\rangle \ll \langle\zeta_S^2\rangle$. Thus, from Eq. (17), $\Delta\mu$ also approaches the flat substrate solution in this limit. However, the effective surface area is larger than the projected area by a factor $(D + 2H)/D$. The coverage is larger by the same factor as shown in Fig. 4 (dotted lines).

At large D the crossover between thin and thick film behaviors is smooth (Fig. 4). At smaller D there is a sharp rise in $\Delta\mu$ followed by a saturation. The rise occurs while the interface remains nearly flat (Fig. 3). Here the value of $\Delta\mu$ is mainly determined by the thickness of the thin regions above the crests of the square wave, $\ell - H/2$. Thus, $\Delta\mu$ changes rapidly with small fractional changes in coverage. When the disjoining pressure exceeds the capillary pressure for penetrating the square grooves, there is a rapid decrease in ℓ at nearly constant $\Delta\mu$ (Figs. 3 and 4).

In recent measurements of N_2 adsorption on rough Ag substrates, an apparent coverage exponent of $\phi = 4.3$ was observed. The increase in ϕ over the flat interface value ($\phi = 3$) was interpreted as evidence for fractal character of the substrate. However, scaling was only obtained

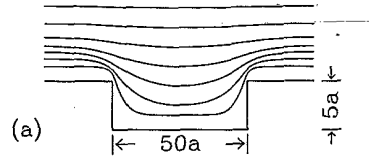

FIG. 3. Calculated liquid surfaces at several mean thicknesses for (a) $D/a = 100$, $H/a = 5$ and (b) $D/a = 10$, $H/a = 5$.

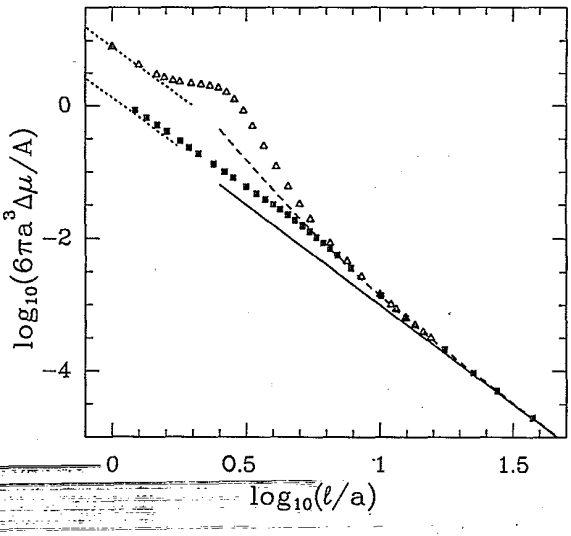

FIG. 4. Chemical potential vs mean thickness for a flat surface (solid line), $D/a = 100$ and $H/a = 5$ (squares), and $D/a = 10$ and $H/a = 5$ (triangles). Dotted lines indicate the limiting thin-film behavior for each case. The dashed line is the Deryagin approximation given by Eq. (17) with $H/a = 5$. Note that $6\pi a^3\Delta\mu/A = (a/l_0)^3$, where l_0 is the equilibrium thickness at $\Delta\mu$ on a flat substrate.

over a factor of 3 in coverage. Our numerical results for simple corrugated (nonfractal) surfaces (e.g., Fig. 4) can be fit to power laws with similar exponents over a comparable range of coverage. Thus, one must be careful about concluding that substrates are fractal. We discuss this issue further in the next section.

Figure 5 compares the first and second Fourier components of the numerical solution with results from the linear and Deryagin approximations. By symmetry, the Fourier transform of the solid profile $\tilde{\zeta}_S(q)$ only contains odd harmonics: $q_j = 2\pi j/D$ with j odd. Linear and Deryagin results for odd j were obtained by multiplying these harmonics by $\tilde{K}(q)(1+q^2\xi^2)^{-1}$ [Eq. (9)] and $(1+q^2\xi^2)^{-1}$ [Eq. (16)], respectively.

Sufficiently thin films follow the underlying solid at a nearly constant distance and $\zeta_L \approx \zeta_S$. In this limit the Deryagin and linear approximations agree well with numerical results. At large film thicknesses, the Deryagin approximation breaks down as discussed above. However, this failure may not be relevant since the liquid surface is already nearly flat in this limit.

The linear approximation fits the numerical data for odd harmonics extremely well when the height is much smaller than the period. When H is greater than or of order D, the linear approximation reproduces the qualitative features of the data but consistently underestimates the roughness. Note that the calculated second harmonic is significant when ℓ is comparable to $H/2$. Like the shift in mean film thickness discussed above, a nonzero second harmonic results from the leading quadratic correction to our linear approximation.[33] The second harmonic is also most noticeable as H/D increases. Care should be used in applying the linear approximation on solid surfaces where changes in height are comparable to the wavelength.

V. SELF-AFFINE AND SELF-SIMILAR SURFACES

The rough solid considered above had a well-defined period. Solid surfaces may also have roughness over a large range of length scales. One class of such surfaces is self-affine surfaces where

$$\langle|\zeta_S(\mathbf{x}+\boldsymbol{\rho}) - \zeta_S(\mathbf{x})|\rangle = b\left|\frac{\rho}{b}\right|^{\beta} \tag{20}$$

with b a characteristic length scale for the roughness and β the roughness exponent.[34] The Fourier spectrum of such a surface scales as $\langle|\tilde{\zeta}_S(q)|^2\rangle \sim q^{-2\beta-d}$, where d is the dimension of the projected surface (d=2 in three dimensions).

In Sec. III A we showed that the liquid interface only followed Fourier components of the substrate at $q < \xi^{-1}$ and $q < \ell^{-1}$. Since self-affine surfaces have roughness at all length scales, only the lower of these two cutoffs is important in determining the dominant features of the interface. For $\ell > a$, this corresponds to $q < \xi^{-1}$. The Deryagin approximation gives this cutoff correctly and we use it to simplify the following discussion. A full treatment produces the same conclusions.

We first consider when our expansion about a flat interface converges. Equation (17) gives the quadratic correction to the film thickness at fixed chemical potential. To test for convergence we compare the size of this correction with Π_d^0. Using the power spectrum for a self-affine solid surface given above, Eq. (20), and the Deryagin

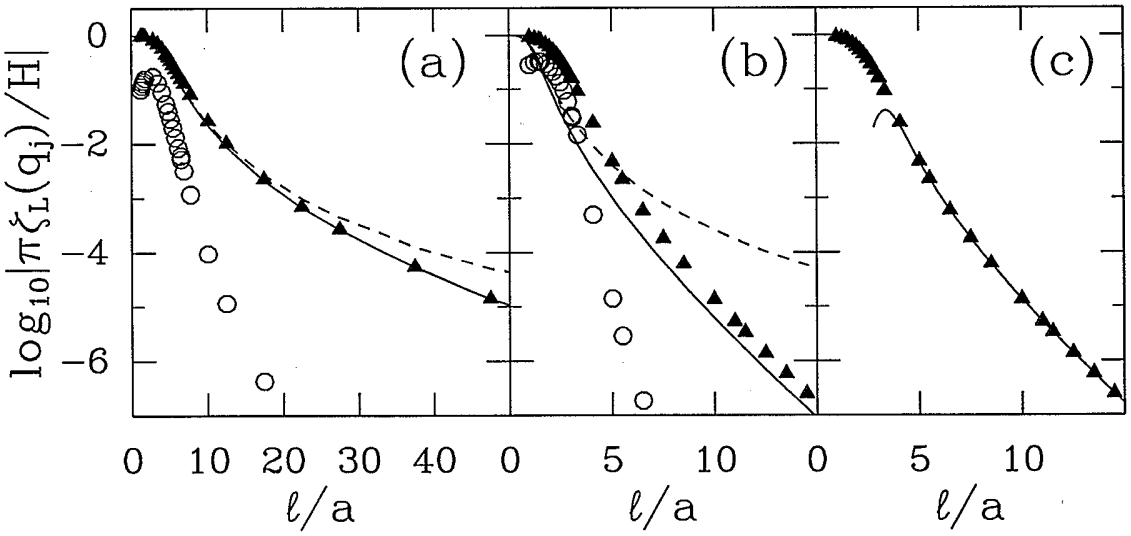

FIG. 5. Calculated variation of $\zeta_L(q_j)$ with ℓ/a for (a) $D/a = 100$, $H/a = 5$ and (b) $D/a = 10$, $H/a = 5$. Numerical results for the first and second harmonics of the solid periodicity are indicated by triangles and circles, respectively. The linear (Deryagin) approximation for the first harmonic is indicated by a solid (dashed) line. Both approximations give zero for the second harmonic. In (c) numerical results for the first harmonic are compared to the linear approximation derived for columnar heterogeneity [Eq. (31)], for $D/a = 10$, $H/a = 5$.

approximation for $\tilde{\zeta}_L/\tilde{\zeta}_S$ we find

$$\langle(\zeta_L-\zeta_S-\ell)^2\rangle \sim \int d^dq\ \frac{q^4\xi^4\langle\tilde{\zeta}_S(q)^2\rangle}{(1+q^2\xi^2)^2}$$

$$\sim \xi^{2\beta}\int d^du\frac{u^{4-2\beta-d}}{(1+u^2)^2}. \qquad (21)$$

For long-ranged power-law potentials [Eq. (10)], $\xi^{2\beta} \sim \ell^{2m\beta}$, and $\partial^2\Pi_d^0/\partial\ell^2 \sim \Pi_d^0/\ell^2$. Thus, the ratio of the second-order correction to the first term in Eq. (17) scales as $\ell^{2m\beta-2}$. For $\beta < m^{-1}$, the correction vanishes in the limit of thick films and the linear approximation is valid. Surface tension dominates at large ℓ and the relation between $\Delta\mu$ and ℓ approaches the flat interface result. For $\beta > m^{-1}$, the correction dominates at large ℓ, and the linear approximation breaks down. In the following we will specialize to $d = 2$, and van der Waals interactions, $m = 2$.

Kardar and Indekeu[25] recently derived similar equations based on the asymptotic form of the energy of a rough surface, and identified the small and large roughness exponent regimes as "weakly" and "strongly" fluctuating, respectively. In the strong-fluctuation regime, roughness remains important in the thick-film limit. Fluctuations with height less than ℓ will be smoothed out, but larger fluctuations will not. The characteristic length of these fluctuations is $\ell^{1/\beta}$ so their curvature is $\ell^{(1-2/\beta)}$. Equating the chemical potential difference to the sum of surface tension and van der Waals terms we find

$$\Delta\mu \sim \frac{\gamma}{b}\left(\frac{\ell}{b}\right)^{1-2/\beta} + \frac{A}{\ell^3}. \qquad (22)$$

In the strong-fluctuation regime, the surface-tension term dominates at large ℓ and the coverage exponent $\phi = 2/\beta - 1$. In the weak-fluctuation regime $\phi = 3$.

If we consider instead the coverage on self-similar fractals, the exponent ϕ can be determined from analogous arguments.[17,25,27,35,36] The volume occupied by a film on the exterior of a fractal (i.e., the coverage) scales as thickness to the power $3 - D_f$, where D_f is the fractal dimension. As noted above, surface tension dominates when the film thickness is larger than a. In this limit, the thickness scales as $\gamma/\Delta\mu$ because smaller features are filled in. The coverage exponent is $\phi = 1/(3 - D_f)$. For thin films ($\ell < a$), surface tension is negligible compared with van der Waals interactions. The thickness of the film scales as $\Delta\mu^{-1/3}$ and the coverage exponent changes to $\phi = 3/(3 - D_f)$.

Pfeifer *et al.*[17] have interpreted recent experimental measurements of N_2 adsorption on Ag as evidence for fractal structure. They found that log-log plots of chemical potential versus coverage lay on straight lines with $\phi = 4.3$ over a factor of 2 or 3 in coverage. They inferred a fractal dimension of $D_f = 2.30 \pm 0.02$ from this value of ϕ, and the relation $\phi = 3/(3-D_f)$ valid in the absence of surface tension. The straight-line behavior occurred over a range of $\Delta\mu$ corresponding to film thicknesses from 8 Å to at most 45 Å on flat surfaces.

This interpretation of the experiments is troubling for several reasons.[25] The first is that Pfeifer *et al.* used the expression for ϕ which neglects surface tension. This expression is only valid for film thicknesses less than $a \approx$ 12 Å, yet experimentally studied thicknesses were larger. If instead the relation $\phi = 1/(3 - D_f)$ valid at large film thicknesses (surface-tension-dominated regime) is used, one finds $D_f = 2.77$ which is unreasonably large.[25,35]

In addition, we remark that coverage curves for *non-fractal* surfaces, e.g., simple corrugated surfaces like those studied in the previous section, fit equally well to straight lines with slope greater than 3 (see Fig. 4). Note that scaling is observed over at most a factor of 3 in coverage in the experiments (200–600 ng/cm^2), while we find apparent scaling over a factor of 3–10. The simple Deryagin approximation valid for any rough surface, Eq. (17), shows a similar straight-line region with $\phi > 3$ (Fig. 4).

Both our numerical results and the measured coverage curves show a crossover to a less steep region at small ℓ. This crossover was identified by Pfeifer *et al.* as the lower length scale cutoff in fractal scaling. Our results suggest that instead it corresponds to the scale where pores are first penetrated. As discussed in the previous section, there is a steep region, $\phi > 3$, at slightly larger ℓ due to the filled pores and a less steep region, $\phi < 3$, at smaller ℓ where the pores empty. The crossover becomes sharper as the ratio of the height of the roughness to the wavelength increases. The effective exponents above and below the crossover become larger and smaller, respectively. At very small ℓ, $\phi \to 3$ once more. This regime would only be observed experimentally if all roughness was at scales greater than the thickness of a monolayer.

Given that the observed scaling can be reproduced by a simple corrugated surface, one cannot conclude from the adsorption experiments that the surface is self-similar or self-affine. Independent scanning-tunneling-microscope results[37] indicating a fractal dimension $D_f = 2.3 \pm 0.1$ over the range 5–50 Å were also cited as supporting evidence. Such measurements cannot reveal overhangs and thus cannot describe self-similar surfaces. Interpreting the measured D_f as the local fractal dimension of a *self-affine* surface one finds $\beta = 3 - D_f = 0.7$. Since this is in the strong-fluctuation regime,[25] the coverage exponent at large ℓ should equal 1.9 which is far from the experimental value. It remains to be seen whether adsorption isotherms can be measured over sufficiently large ranges of coverage to definitively identify fractal scaling.

VI. WETTING ON HETEROGENEOUS SOLIDS

We now consider the case of a solid with a flat interface, $\zeta_S(\mathbf{x}) = 0$, but with heterogeneous composition, i.e., spatially varying potentials u_{SV}, u_{SL}. If these fluctuations only affect the strength of the coupling rather than its functional form, we can write $w(\mathbf{r},\mathbf{r}') = \epsilon(\mathbf{r}')\,w_0(\mathbf{r}-\mathbf{r}')$ where $\epsilon(\mathbf{r}')$ describes the solid composition at point $\mathbf{r}'$. The normalization of the average interaction w_0 is chosen

so that $\langle \epsilon(\mathbf{r}') \rangle = 1$.

A general linear approximation can be derived following Sec. III A. We specialize to two simple geometries: (i) layered systems where ϵ only depends on z'; (ii) columnar systems where $\epsilon(\mathbf{r}') - 1 = \phi(\mathbf{x}')f(z')$ is separable.[38] As before we present detailed results for van der Waals interactions where variations in ϵ correspond to fractional changes in the Hamaker constant.

A. Layered solids

The layered geometry is appropriate for artificially structured materials grown by deposition. Recent experimental techniques allow precise control of the composition along the growth direction to achieve desired electronic, magnetic, and mechanical properties. Symmetry requires that the surface of a liquid wetting such a structure be flat, $\zeta_L = \ell$. However, the layered structure will change the variation of Π_d with ℓ, and hence the equilibrium thickness ℓ. From Eq. (1)

$$\Pi_d(\mathbf{x}, \zeta_L(\mathbf{x})) = \int_{-\infty}^{0} dz' \, \epsilon(z') \int d^2\rho \, w_0(\boldsymbol{\rho}, \ell - z'). \tag{23}$$

For nonretarded van der Waals interactions, $w_0(\rho, z) = A_0\pi^{-2}(\rho^2+z^2)^{-3}$, and the final integral can be evaluated for any given $\epsilon(z')$:

$$\Pi_d(\ell) = \frac{A_0}{6\pi\ell^3} \int_{-\infty}^{0} dz' \frac{3\epsilon(z')}{\ell(1 - z'/\ell)^4} \equiv \frac{A_{\text{eff}}}{6\pi\ell^3} \, . \tag{24}$$

The effective Hamaker constant A_{eff} at a given film thickness is thus A_0 times a weighted average of $\epsilon(z')$. The weighting function, $(3/\ell)(1 - z'/\ell)^{-4}$, falls off rapidly for $z' < -\ell$. If the first layer of the solid is thicker than ℓ, one may to a good approximation ignore successive layers. If ℓ is larger than the size of layers, one must include all layers.

Suppose that the solid consists of consecutive layers of uniform Hamaker constant A_i which terminate at successive depths ℓ_i below the surface. Then integrating Eq. (24) yields

$$\Pi_d(\ell) = \frac{1}{6\pi} \left(\frac{A_1}{\ell^3} + \frac{A_2 - A_1}{(\ell + \ell_1)^3} + \frac{A_3 - A_2}{(\ell + \ell_2)^3} + \cdots \right) \, . \tag{25}$$

The first term represents the chemical potential for a uniform solid of Hamaker constant A_1. The second term represents the correction for a solid which changes to Hamaker constant A_2 for $z' < -\ell_1$. Subsequent terms represent similar corrections.

B. Columnar solids

If A varies along the solid surface, the liquid interface roughens.[39] In practice, such surfaces could be made from cross-sectional slices through the layered structures just discussed. We consider the more general case where the fluctuations are separable, $\epsilon(\mathbf{r}') - 1 = \phi(\mathbf{x}')f(z')$. Then the disjoining pressure [Eq. (4)] becomes

$$\Pi_d(\mathbf{x}, \zeta_L(\mathbf{x})) = \int d^2\rho \int_{\zeta_L}^{\infty} dz' \, w_0(\boldsymbol{\rho}, z) \times [1 + \phi(\mathbf{x} + \boldsymbol{\rho}) f(\zeta_L - z')] \, . \tag{26}$$

As in Sec. III A we expand about a flat interface solution, $\langle \zeta_L \rangle = \ell$. To first order in $|\zeta_L(\mathbf{x}) - \ell|$ and $\epsilon - 1$

$$\Pi_d(\mathbf{x}, \zeta_L(\mathbf{x})) = \Pi_d^0(\ell) + \int d^2\rho \, \phi(\mathbf{x} + \boldsymbol{\rho}) W_0(\boldsymbol{\rho}) \cdot - [\zeta_L(\mathbf{x}) - \ell] \int d^2\rho w_0(\boldsymbol{\rho}, \ell), \tag{27}$$

where

$$W_0(\boldsymbol{\rho}) = \int_{\ell}^{\infty} dz \, w_0(\boldsymbol{\rho}, z) \, f(\ell - z). \tag{28}$$

The average thickness ℓ is given by Eq. (5), and the fluctuations of the liquid interface satisfy

$$\xi^2 \nabla^2 \zeta_L(\mathbf{x}) = \zeta_L(\mathbf{x}) - \ell - \int d^2\rho \, G(\mathbf{x} - \boldsymbol{\rho}) \, \phi(\boldsymbol{\rho}), \tag{29}$$

where the kernel G is

$$G(\mathbf{x}) = \frac{W_0(\mathbf{x})}{\int d^2\boldsymbol{\rho} \, w_0(\boldsymbol{\rho}, \ell)} = \frac{\xi^2(\ell)}{\gamma} W_0(\mathbf{x}). \tag{30}$$

As before, the linear equation is solved by Fourier transformation and we find

$$\tilde{\zeta}_L(q) = \frac{\tilde{\phi}(q) \, \tilde{G}(q)}{1 + \xi^2 q^2} \, . \tag{31}$$

Note that ξ plays the same role as in Sec. III A. Changes in the solid composition ϕ on wavelengths smaller than ξ are strongly attenuated. The form of $\tilde{G}$ is somewhat different from $\tilde{K}$, in particular it has units of length and $\tilde{G}(0) \neq 1$. Notice that it can be written as a weighted average of the kernel found for rough solids:

$$\tilde{G}(q) = \xi(\ell)^2 \int_{\ell}^{\infty} dz \, \xi(z)^{-2} \tilde{K}(q, z) f(\ell - z). \tag{32}$$

To determine G's role we consider the case of van der Waals interactions where the variation in the solid composition is only along the $\mathbf{x}$ direction: $f(z) = 1$. For nonretarded van der Waals interactions, $\tilde{K}$ is given by Eq. (13) with $m = 2$. Since $\tilde{K}(q = 0)$=1, Eq. (32) yields $\tilde{G}(0) = \ell/3$. In the limit of large ℓ the asymptotic form $\tilde{K} \sim (q\ell)^{3/2} \exp(-q\ell)$ can be used. Integrating Eq. (32) then yields $\tilde{G} \sim \ell(q\ell)^{1/2} \exp(-q\ell)$ at large $q\ell$. Hence Fourier components at wavelengths smaller than ℓ are exponentially damped. As before, a Deryagin approximation would leave out this nonlocal term.

The square corrugation treated numerically in Sec. IV can also be described as columnar heterogeneity. The solid surface (z=0) is defined to coincide with the crests of the square wave. The function ϕ is then zero over the crests of the square waves and -1 over the troughs, and $f(z)$ is the Heaviside function $\Theta(H + z)$. Thus Eq. (32)

yields

$$\tilde{G}(q) = \tfrac{1}{2}q^3\ell^4 \int_{q\ell}^{q(\ell+H)} du\, u^{-2}K_2(u)\ . \qquad (33)$$

For small qH and H/ℓ this kernel reduces to that obtained in Sec. III A. In Sec. IV we saw that the rough surface approximation differed from the numerical results for large H/D. Since $qH = 2j\pi H/D$ for the jth harmonic of the square wave, this result is no longer surprising. The small parameter in the chemical heterogeneity expansion $\zeta_L - \ell$ is intrinsically smaller than that in the rough surface expansion $|\zeta_L(\mathbf{x})-\ell-\zeta_S(\mathbf{x}+\rho)|$. As shown in Fig. 5(c) the chemical heterogeneity results for the first harmonic are indistinguishable from the numerical results for $\ell/a > 4$.

VII. DISCUSSION

In this paper we have developed equations for the equilibrium conformation of thin liquid films wetting rough or chemically heterogeneous solid surfaces. These equations were solved numerically for van der Waals interactions on simple corrugated surfaces. Linear approximations were derived for general interactions and disorder.

One important length scale which emerges from the analytic and numerical results is the *healing length*, ξ. It embodies the competition between the long-range attractive potential $w(\mathbf{r},\mathbf{r}')$, which favors following the solid surface on wavelengths larger than ξ, and the surface tension γ, which has a smoothing effect for smaller wavelengths. Since the potential falls off with distance, ξ increases with film thickness. In the linear approximation, the ratio of Fourier components of the liquid surface to those of the solid heterogeneity falls off as a Lorentzian for wavelengths $q > \xi^{-1}$.

The healing length is the only scale that arises in the Deryagin approximation, where the disjoining pressure is approximated by a function of the local film thickness. Nonlocal effects included in the full linear theory lead to additional smoothing for wavelengths less than the mean film thickness ℓ. For power-law potentials, an entire region of the surface with size ℓ contributes nearly equally to the disjoining pressure at each point. The effect of heterogeneity at smaller wavelengths $q < \ell^{-1}$ is exponentially damped. Other potentials show similar or even faster damping and are considered in the Appendix.

Heterogeneity of the solid surface will only be followed by the liquid film at wavelengths larger than both ξ and ℓ. The larger of the two lengths plays the dominant role in smoothing the film. For any potential, ℓ is the larger length at small film thickness and ξ becomes larger for thick films. For power-law potentials, this crossover occurs at the microscopic length a. The Deryagin approximation may provide an adequate approximation for thick films in some cases.

Our prediction for the correlations between the structure of the solid surface and the liquid-air interface can be verified most directly by x-ray reflection and grazing incidence diffraction techniques.[13,14] The major experimental results reported so far are independent values for the total rms roughness of the substrate and liquid interfaces. The rms fluctuation of the liquid interface was found to be intermediate between the solid roughness and the thermal roughness of the bulk fluid. As predicted above, the liquid roughness was larger in thin films (ℓ=14 Å) than in thick films (ℓ=70–100 Å). The predicted correlation in the phase of Fourier components of the solid and liquid interfacial roughness [Eq. (9)] was confirmed qualitatively with off-axis scattering measurements.[13] The advantage of scattering measurements for future studies is that each Fourier component of the liquid interfacial roughness can be independently compared to the corresponding component of the solid roughness. Thus, our Eq. (9) can be tested experimentally.

Microscopic imaging ellipsometry has also been used to examine local fluctuations in the film thickness for PDMS liquids. It was observed that the rms fluctuation of the liquid surface varies as $1/\ell$, where ℓ is the local film thickness.[15] We have verified[40] that the linear theory (Sec. III) predicts that the liquid surface roughness scales in this manner in the limit of weak roughness. Additional experiments can be done on precursor films of advancing liquid drops. In such a setup, the average film thickness is a smoothly varying function of position and the dependence of the local roughness on this parameter can be tested as well.

Experiments have also probed the effect of solid heterogeneity on adsorption isotherms where the coverage is measured as a function of the vapor pressure or chemical potential. We have studied the effect of roughness on isotherm measurements through exact numerical solutions and an extension of the Deryagin approximation to second order, Figs. 3–5. For the case of attractive potentials considered here, roughness increases the film thickness at fixed chemical potential. Even the coverage exponent ϕ relating the film volume (thickness) to the chemical potential may increase in the extreme cases of self-similar fractal surfaces or strongly fluctuating self-affine surfaces.

Recent measurements of N_2 adsorption on flash-deposited Ag showed[17] an apparent change of the coverage exponent, which was interpreted as evidence of fractal structure. An important conclusion of our work is that care must be taken in making such interpretations. Even nonfractal surfaces with a single characteristic length scale show an apparent increase in ϕ over up to an order of magnitude in coverage. Similar deviations from the simple $\Delta\mu \sim \ell^{-3}$ power law may occur for *any* irregular (nonfractal) surface.

Several important issues have not been discussed in the present paper. One is the effect of thermal fluctuations on the liquid interface.[18,40,41] Such fluctuations clearly provide a lower bound on the measured roughness. The smoothing of the interface with increasing film thickness described above will only be observable when the disorder-induced roughness is appreciable compared

to the thermal roughness.

We have also neglected the discrete nature of the liquids. For example, the film thickness cannot be less than a monolayer. At molecular scales the form of interatomic forces also becomes more complicated and a continuum theory as the one employed here breaks down. Depending on the form of the potential one may either find that at least a monolayer covers the surface, or that the film ruptures.

Rupture is even more important in the case of repulsive long-range interactions which was not treated here. If the potential w is negative at large distances, ξ^2 may be less than zero. This leads to singularities in our linear approximation when $q\xi$ is of order unity [Eq. (9)]. The mean film thickness at fixed $\Delta\mu$ will be *decreased* by roughness (Sec. III B). These changes reflect the inherent instability of nonwetting films which must eventually lead to rupture. Note that negative values of w do not necessarily imply that the liquid is nonwetting, there may be a very strong short-range attraction.[42] A rich variety of behavior may occur when the potential changes sign.

ACKNOWLEDGMENTS

We thank J. Harden, M. Kardar, J. Krim, and E. Raphael for useful discussions. One of us (M.O.R.) acknowledges support from National Science Foundation (NSF) Grant No. DMR85-53271, and the Sloan Foundation. Another (D.A.) acknowledges support from the Israel Academy of Sciences and Humanities and the U.S.–Israel Binational Science Foundation under Grant No. 87-00338. Support from NSF under Grant No. PHY82-17853 at the University of California in Santa Barbara is also acknowledged.

APPENDIX: LINEAR RESPONSE FOR EXPONENTIAL AND GAUSSIAN POTENTIALS

The power-law potential discussed in Sec. III A has no intrinsic length scale. Thus ℓ is the only length which can appear in $\tilde{K}$. As one example of a potential with an intrinsic length we take an exponential

$$w(r) = C\exp(-r/b). \tag{A1}$$

From Eqs. (7) and (8) we find

$$\xi^2 = \frac{a'^4}{b(b+\ell)}\exp\left(\frac{\ell}{b}\right), \tag{A2}$$

$$\tilde{K}(q) = \frac{\ell\sqrt{1+(qb)^2}+b}{(\ell+b)[1+(qb)^2]^{3/2}} \times \exp\left(-\frac{\ell}{b}[\sqrt{1+(qb)^2}-1]\right), \tag{A3}$$

where $a' = (\gamma/2\pi C)^{1/4}$ is now the relevant microscopic length. Thus, ξ is nearly constant for $\ell < b$ and increases exponentially for $\ell \gg b$ as the potential rapidly decreases. For $qb \gg 1$, $\tilde{K}(q) \sim \exp(-q\ell)/(qb)^2$. Thus the exponential cutoff at large q is the same as for power-law potentials. For $\ell > b$ there is an intermediate range $\ell^{-1} < q < b^{-1}$ where $\tilde{K}(q) \sim \exp(-\frac{1}{2}q^2\ell b)$.

Similarly, the integrals for a Gaussian potential,

$$w(r) = C\exp(-r^2/b^2), \tag{A4}$$

are readily evaluated to yield

$$\xi^2 = \frac{\gamma}{C\pi b^2}\exp\left(\frac{\ell^2}{b^2}\right), \tag{A5}$$

$$\tilde{K}(q) = \exp[-\tfrac{1}{4}(qb)^2]. \tag{A6}$$

Note that for this special case the cutoff at large q no longer depends on the film thickness.

Two general features are indicated by these results. The first is that the more rapidly the pair potential falls off, the more rapidly ξ increases. Thus the crossover to the surface-tension dominated regime occurs at smaller film thicknesses. The second is that steeper potentials lead to a more rapid decay of $\tilde{K}(q)$ at large q.

[1] J. N. Israelachvili, *Intermolecular and Surface Forces* (Academic, New York, 1985).
[2] R. Hunter, *Foundations of Colloid Science* (Clarendon, New York, 1987).
[3] B. V. Deryagin, N. V. Churaev, and V. M. Muller, *Surface Forces* (Consultants Bureau, New York, 1987).
[4] P.-G. de Gennes, Rev. Mod. Phys. **57**, 827 (1985).
[5] *Contact Angle, Wettability and Adhesion*, Advanced Chemistry Series, Vol. 43, edited by F. M. Fowkes (American Chemical Society, Washington, D.C., 1964).
[6] *Wetting, Spreading and Adhesion*, edited by J. F. Padday (Academic, New York, 1978).
[7] For a review see, e.g., J. Villain, in *Scaling Phenomena in Disordered Systems*, edited by R. Pynn and A. Skjeltorp (Plenum, New York, 1985); T. Nattermann and J. Villain, Phase Transitions **11**, 5 (1988).
[8] Y. Pomeau and J. Vannimenus, J. Coll. Interface Sci. **104**, 477 (1985).
[9] J.-F. Joanny, and P.-G. de Gennes, J. Chem. Phys. **81**, 552 (1984).
[10] M. O. Robbins and J.-F. Joanny, Europhys. Lett. **3**, 729 (1987).
[11] D. Andelman, J.-F. Joanny, and M. O. Robbins, Europhys. Lett. **7**, 731 (1988).
[12] V. M. Starov and N. V. Churaev, Coll. J. (USSR) **39**, 7 (1977).
[13] S. Garoff, E. B. Sirota, S. K. Sinha, and H. B. Stanley, J. Chem. Phys. **90**, 7505 (1989).

[14] J. Daillant, J. J. Benattar, L. Bosio, and L. Leger, Europhys. Lett. **6**, 431 (1988); J. Daillant, J. J. Benattar, and L. Leger, Phys. Rev. A **41**, 1963 (1990).
[15] D. Beaglehole, J. Phys. Chem. **93**, 893 (1989).
[16] F. Heslot, N. Fraysse, and A. M. Cazabat, Nature (London) **338**, 640 (1989).
[17] P. Pfeifer, Y. J. Wu, M. W. Cole, and J. Krim, Phys. Rev. Lett. **62**, 1997 (1989).
[18] A. Braslau, M. Deutsch, P. S. Pershan, and A. H. Weiss, Phys. Rev. Lett. **54**, 114 (1985).
[19] W. A. Steele, *The Interaction of Gases with Solid Surfaces* (Pergamon, Oxford, 1974).
[20] Self-similar fractal surfaces necessarily have overhangs and cannot be treated in this way.
[21] $\tilde{\zeta}_L(\mathbf{q})$ is the Fourier transform of $\zeta_L(\mathbf{x}) - \ell$.
[22] Within a perturbation theory, the Lifshitz theory for van der Waals forces between two rough solid surfaces was treated by P. Mazur and A. Maradudin, Phys. Rev. B **22**, 1677 (1980); **22**, 279 (1981).
[23] E. Cheng and M. W. Cole, Phys. Rev. B **38**, 987 (1988).
[24] In particular, the phases can no longer be treated as continua, and short-range contributions to the interparticle force become larger than the van der Waals interaction.
[25] M. Kardar and J. O. Indekeu, Europhys. Lett. **12**, 161 (1990); Phys. Rev. Lett. **65**, 662 (1990).
[26] A. C. Levi and E. Tosatti, Surf. Sci. **178**, 425 (1986).
[27] P.-G. de Gennes, in *Physics of Disordered Materials*, edited by D. Adler, H. Fritzsche, and S. R. Ovshinsky (Plenum, New York, 1985), p. 227.
[28] B. Deryagin, Kolloidn. Zh. **17**, 827 (1955).
[29] Note that the Deryagin approximation is traditionally used in calculating the interaction between simple curved surfaces such as crossed cylinders rather than between rough surfaces. In this context the approximation is accurate at separations small compared to the radii of curvature. This corresponds to the condition $q\ell < 1$ found in the text.
[30] An expansion to second order around the local Deryagin approximation has been performed in Ref. 41. It agrees with expanding our $K(q)$ to second order in q around $q = 0$.
[31] For any roughness the integral over z can be performed analytically.
[32] Our definition of the coverage exponent ϕ is equal to $1/\psi$ of Ref. 25 and to m of Ref. 35.
[33] The origin of this component is most easily seen for thin films. For the solid, symmetry between the crests and troughs causes $\tilde{\zeta}_S(q_2)$ to vanish. For small ℓ/a the liquid interface follows a little above the solid. The crests are slightly longer and the troughs are shorter by a similar amount. This breaks the symmetry and gives a finite $\tilde{\zeta}_L(q_2)$. For $D/H \gg 1$ this is a small effect, but for smaller D/H it becomes substantial.
[34] See, for example, J. Feder, *Fractals* (Plenum, New York, 1988).
[35] P. Pfeifer and M. W. Cole, New J. Chem. **14**, 221 (1990); P. Pfeifer, M. W. Cole, and J. Krim, Phys. Rev. Lett. **65**, 663 (1990).
[36] F. Brochard, C. R. Acad. Sci. (Paris) **304II**, 785 (1987).
[37] P. Pfeifer, J. Kenntner, J. L. Wragg, J. West, H. W. White, J. Krim, and M. W. Cole, Bull. Am. Phys. Soc. **34**, 728 (1989), and unpublished.
[38] The effect of a similar type of disorder on critical and first-order wetting transitions has been considered by G. Forgacs, H. Orland, and M. Schick, Phys. Rev. B **32**, 4683 (1990).
[39] The specific case of two half planes with differing Hamaker constant was considered in M. W. Cole and E. Vittoratos, J. Low Temp. Phys. **22**, 223 (1976).
[40] J. L. Harden and D. Andelman (unpublished).
[41] J. L. Harden and R. F. Kayser, J. Coll. Interface Sci. **127**, 548 (1989).
[42] F. Brochard, J. M. Di Meglio, D. Quéré and P.-G. de Gennes, Langmuir (to be published).